Moringa oleifera ethanolic extract attenuates tilmicosin-induced renal damage in male rats via suppression of oxidative stress, inflammatory injury, and intermediate filament proteins mRNA expression

Shimaa M. Abou-Zeid [a], Amany I. Ahmed [b], Ashraf Awad [c,*], Wafaa A. Mohammed [d], Mohamed M.M. Metwally [e], Rafa Almeer [f], Mohamed M. Abdel-Daim [f,g], Samah R. Khalil [h]

[a] *Forensic Medicine and Toxicology Department, Faculty of Veterinary Medicine, University of Sadat City, 32897, Egypt* [b] *Biochemistry Department, Faculty of Veterinary Medicine, Zagazig University, 44511, Egypt*
[c] *Animal Wealth Development Department, Faculty of Veterinary Medicine, Zagazig University, 44511, Egypt* [d] *Clinical Pathology Department, Faculty of Veterinary Medicine, Zagazig University, Egypt* [e] *Pathology Department, Faculty of Veterinary Medicine, Zagazig University, 44511, Egypt*
[f] *Department of Zoology, College of Science, King Saud University, P.O. Box 2455, Riyadh 11451, Saudi Arabia* [g] *Pharmacology Department, Faculty of Veterinary Medicine, Suez Canal University, Ismailia 41522, Egypt* [h] *Forensic Medicine and Toxicology Department, Faculty of Veterinary Medicine, Zagazig University, 44511, Egypt*

ARTICLEINFO

Keywords:
Tilmicosin
Moringa oleifera
Intermediate filament protein
Nestin
Desmin
Vimentin

ABSTRACT

Tilmicosin (Til) is a popular macrolide antibiotic, widely used in veterinary practice. The present study was designed to address the efficacy of *Moringa oleifera* ethanolic extract (MOE) in protecting against Tilmicosin (Til) - induced nephrotoxicity in Sprague Dawley rats. Animals were treated once with Til (75 mg/kg bw, subcutaneously), and/or MOE for 7 days (400 or 800 mg/kg bw, by oral gavage). Til-treatment was associated with significantly increased serum levels of creatinine, urea, sodium, potassium and GGT activity, as well as decreased total protein and albumin concentrations. Renal tissue hydrogen peroxide (H_2O_2) and malondialdehyde (MDA) levels were elevated, while the activities of superoxide dismutase (SOD) and glutathione peroxidase (GPx) enzymes were diminished. The levels of renal tumor necrosis factor alpha (TNF-α) and interleukin-1 beta (IL-1β) and the mRNA expression of intermediate filament protein encoding genes (desmin, nestin and vimentin) in the kidney were up- regulated with histopathological alterations in renal glomeruli, tubules and interstitial tissue. These toxic effects were markedly ameliorated by co-treatment of MOE with Til, in a dose dependent manner. Taken together, these results indicate that MO at 800 mg/kg protects against Til-induced renal injury, likely by its potent antioxidant and anti-inflammatory properties, which make it suitable to be used as a protective supplement with Til therapy.

1. Introduction

Tilmicosin (Til) is a broad-spectrum semisynthetic macrolide antibiotic derived from tylosin. Because Til reaches high concentrations in the lung tissue, it is efficiently used for the treatment of bovine and ovine respiratory disease caused by *Mannheimia haemolytica, Pasteurella multocida, Mycoplasma spp., staphylococci* and *streptococci*. It is used in feedlot calves to reduce the prevalence of respiratory disease and improve growth, and was approved for the treatment of swine respiratory disease caused by *Pasteurella multocida* and *Actinobacillus pleuropneumoniae* and for the treatment of rabbit pasteurellosis [1,2]. Further, it is effectively used to treat cow mastitis [3] and mycoplasmosis in chicken [4].

Til therapy may be associated with some side effects in case of misuse or improper administration, mainly, the cardiotoxic effect mediated via depletion of cardiac intracellular calcium, resulting in a negative inotropic effect [1]. Previous experiments demonstrated hematological changes and hepatoxicity in Til-treated rats and broiler chicken as evidenced by elevated blood transaminases, ALP and LDH activities, and total bilirubin level [5–7]. Additionally, a reduction in the protein profile was recorded in rats [5], mice [8], and chicken [7]. Increasing evidence shows that Til demonstrated cardiotoxicity with marked fatalities especially in horses, goats, swine and even in human [1,9].

Moreover, the nephrotoxicity of Til was evidenced biochemically by elevated serum urea and creatinine levels that have been previously reported in rats [5,6], mice [10], and broiler chicken [7]. Histopathologic investigations revealed a congestion of the intertubular blood vessels with the presence of eosinophilic material inside the lumen of renal tubules of Til-treated rats [6]. However the mechanisms underlying Til-induced nephrotoxicity are still far from clear, the modulations of the oxidant/antioxidant status are suggested, as Til was reported to induce oxidative stress with depletion of antioxidant defense mechanisms in the liver and heart of treated animals [5,11,12].

Inflammation could also play a role in Til-induced renal tissue injury, because oxidative stress and inflammation contribute to fuel each other and thereby establishing a vicious cycle that propagates the inflammatory response and oxidative injury [13,14]. The mechanism by which inflammation might amplify the initial oxidant stress remained unclear until recent studies provided some insights. All stages of the inflammatory response are affected by oxidative stress,

* Corresponding author.
E-mail addresses: shima10_a@yahoo.com (S.M. Abou-Zeid), drmonmon_vet@yahoo.com (A.I. Ahmed), afsawad@zu.edu.eg (A. Awad), waffa.clinical@yahoo.com (W.A. Mohammed), metywally@gmail.com (M.M.M. Metwally), ralmeer@ksu.edu.sa (R. Almeer), abdeldaim.m@vet.suez.edu.eg (M.M. Abdel-Daim), dr_ samahkhalil@yahoo.com, resamah@zu.edu.eg (S.R. Khalil).

https://doi.org/10.1016/j.biopha.2020.110997
Received 10 September 2020; Received in revised form 24 October 2020; Accepted 8 November 2020
Available online 13 November 2020
0753-3322/© 2020 The Authors. Published by Elsevier Masson SAS. This is an open access article under the CC BY-NC-ND license (http://creativecommons.org/licenses/by-nc-nd/4.0/).

including the release of molecules acting as endogenous danger signals from damaged tissues, activation of immune receptors and stimulation of the signaling pathways starting the adaptive cellular response to such noxious signals [15].

Researchers have been actively searching for safe protective agents to avoid the deleterious effects induced by Til treatment. Medicinal plants are widely used globally in addressing such indispositions due to their low cost, availability and minimal side effects with safe therapeutic efficiency [16–18]. Among them, *Moringa oleifera* (MO) Lam. (Family: Moringaceae) is a rapidly growing arbor, 5− 10 m height, in tropical and subtropical countries. Almost every part of the plant is of value in one way or another. In many countries, MO is processed in different ways and consumed as a dietary supplementary or vegetables [19]. The leaves ethanolic extract has an oral LD_{50} value of 5585 mg/kg in rats [20]; therefore, it has a wide safety margin and low toxicity. The antioxidant content of the plant was previously acknowledged, as it has effectively protected the cellular biomolecules from the oxidative damage caused by free radicals [12,21,22]. Interestingly, the MO plant was reported to have anticarcinogenic, antidiabetic, anti-inflammatory, anti-atherosclerotic, anti-apoptotic, hepatoprotective, neuroprotective, and cardioprotective activities [17,19,23–28].

Podocytes are visceral epithelial cells located on the glomerular basement membrane as the terminal element in the filtration. As podocytes are affected at the early stage of glomerular damage [29], estimation of the intermediate filament (IF) proteins desmin, nestin and vimentin as biomarkers of podocyte injury, is quite important to quantitatively detect early glomerular disorders.

The present study was aimed to explore the role of MOE in attenuating the toxic insult induced by Til treatment, where the oxidative stress and inflammation could be involved in the pathophysiology of Til- induced nephrotoxicity. This aim was affirmed by studying renal function, oxidative stress, antioxidant status, and inflammatory biomarkers, as well as the mRNA expression of glomerular podocyte markers (desmin, nestin and vimentin). Additionally, a quantitative assessment of the renal histomorphological alterations was conducted.

2. Materials and methods

2.1. Chemicals

Tilmicosin ($C_{46}H_{80}N_2O_{13}$) antibiotic (Til) was purchased from Elanco Animal Health (USA) as a commercial preparation containing 300 mg tilmicosin phosphate/mL. *Moringa oleifera* (MO) leaves were obtained as a gift from the Egyptian Scientific Society of Moringa, National Research Center, Egypt. The plant was botanically identified by Prof. Dr. Abou El-Fetoh M. Abd-Allah, Chairman of the Society.

2.2. Preparation of the ethanolic extract of Moringa oleifera leaves

Moringa oleifera leaves ethanolic extract (MOE) was prepared by drying the clean leaves for 3 weeks at room temperature followed by grinding into a fine powder with a high-speed milling machine. One kg of the obtained powder was extracted for 48 h in one liter of absolute ethanol, followed by two rounds of filtration through filter paper (2 µm-sized pores). The resulting extract was evaporated using a rotary evaporator at 50 °C. The obtained residue from 1 kg dried powder was 78.3 g that was reconstituted in distilled water at the beginning of the experiment and was kept in a brown bottle at 4 °C all over the experimental period.

2.3. Gas chromatography/mass spectrometry analysis (GC–MS) of MOE

The analysis of MOE was performed using a Trace GC 1310-TSQ mass spectrometer (Thermo Scientific, Austin, TX, USA) with a direct capillary column TG–5MS (30 m x0.25 mm x0.25 µm film thickness) [18]. Detection of the individual components was based on comparing their retention times and mass spectra with those of two commercial libraries; the National Institute of Standards and Technology (NIST) mass spectral library, containing the EI spectra of more than 200,000 compounds (213,000 spectra), and the Wiley Registry, containing the EI spectra of almost 600,000 unique compounds (662,780) [30].

2.4. Animals and treatment

All animal procedures were approved in advance (ZU-IACUC/2/F/ 80/2019) by the Institutional Animal Care and Use Committee of Zagazig University, Egypt, which were performed in accordance with the animal care and handling guidelines of the National Institutes of Health (NIH). Sixty adult male Sprague–Dawley rats (180–190 gm) were obtained from the Laboratory Animal Farm, Faculty of Veterinary Medicine, Zagazig University, Egypt, and were acclimated in our facility for 2 weeks. Animals were caged at standardized conditions (12 h light/ dark period; temperature 23 ± 2 °C; humidity 50 %) with free access to food and water during the acclimatization period and throughout the experiment. Animals were randomly allocated into six groups, 10 rats each. Initial body weights of all animals were recorded for adjustment of doses of MOE and Til.

Animals of the control group were injected once subcutaneously (S/ C) with normal saline (Control, 1st group). MOE was administered by oral gavage to the 2nd and 3rd groups at 400 (MOE-L) or 800 (MOE-H) mg/kg bw, respectively, for 7 days. The 4th group was subcutaneously (S/C) injected with Til at a single dose of 75 mg/kg bw. The 5th and 6th groups received a single injection of Til at a dose of 75 mg/kg bw, followed by oral administration of MOE at 400 (Til/MOE-L) or 800 (Til/ MOE-H) mg/kg bw, respectively. Administration of MOE to both Til/ MOE-L and Til/MOE-H was done following a single Til injection with an hour interval and was continued for another 6 successive days without Til injection. The time point for sacrifice was at the 7th day of S/ C injection of Til. The dose of Til injected in the current study was determined based on the results of a previous dose-dependent work [12], where it induced a significant tissue damage via oxidative stress and apoptosis. The selection of ethanolic extract of MO leaves levels was based on the previous studies that demonstrated the role of MOE in enhancing the protective activity of the antioxidant system and slowing the pathological development of tissue alterations induced by xenobiotic exposure [12,21]. *2.5. Serum and kidney sampling*

Mortalities were recorded throughout the experimental work. At the indicated time point, the body weights of individual animals were recorded and blood samples were collected from the retro-orbital plexus. Samples were allowed to sit for 30 min, then centrifuged at 3000 rpm at 4 °C for 15 min, and sera were collected and stored at − 20 °C to be used for estimation of physiological biomarkers. Under sodium pentobarbital anesthesia (60 mg/kg), animals from all groups were euthanized by cervical dislocation. The dissected kidneys were assigned into two sets. The first set was homogenized in cold PBS (pH 7.4) using Teflon homogenizer. The homogenates were centrifuged at 14,000×g for 20 min at 4 °C. The obtained supernatant was then stored at − 80 °C until be used for

assessment of oxidative stress, antioxidant status and inflammatory biomarkers. The other set of kidney samples was frozen immediately in liquid nitrogen and stored at − 80 °C until the processing for RT-qPCR analysis to evaluate the expression of intermediate filament proteins.

2.6. Serum physiological biomarkers

Serum creatinine, urea, total protein, albumin, sodium, potassium and gamma glutamyl transferase (GGT) were estimated spectrophotometrically, as renal function biomarkers, using standard kits obtained from Biodiagnostic Co., Giza, Egypt, following the manufacturer's instructions.

2.7. Oxidative stress/antioxidant biomarkers

Renal hydrogen peroxide (H_2O_2) level was assessed using colorimetric assay kit Catalog No. MBS841818; MyBioSource, San Diego, United States. The concentration of the lipid peroxidation product malondialdehyde (MDA), and the activities of superoxide dismutase (SOD) and glutathione peroxidase (GPx) were measured in renal tissue using assay kits (Catalog No. MD2529, SD2521, GP2524, respectively), Biodiagnostic Co. Giza, Egypt, per the manufacturer's instruction.

2.8. Inflammatory response markers

Tumor necrosis factor-alpha (TNF-α) and interleukin-1 beta (IL-1β) were quantified using the commercial rat enzyme - linked immunosorbent assay (ELISA) kits obtained from MyBioSource, San Diego, California, USA (Catalog No: MBS2507393, MBS825017, respectively). The assessment protocols were followed as provided by the manufacturer.

2.9. Transcription levels of intermediate filament proteins (desmin, nestin and vimentin)

RNeasy Mini Kit and Reverse Transcription kit (Qiagen, Heidelberg, Germany) were used for extraction of total RNA from kidney tissue and reverse transcription of the first-strand cDNA, following the manufacturer's instructions. Real-time qPCR was performed on a Rotor-Gene Q cycler (Qiagen, Germany) using QuantiTect SYBR Green PCR kits (Qiagen, Heidelberg, Germany) and forward and reverse primers for each gene, as displayed in Table 1. Relative fold changes in the expression of target genes were calculated using the comparative $2-\Delta\Delta$Ct (Ct: cycle threshold) method [34] with Glyceraldehyde- 3-Phosphate Dehydrogenase (GAPDH) gene as an internal control to normalize target gene expression levels.

Table 1

Genes	Forward (5′-3′)	Reverse (5′-3′)	References
Desmin	CCAACTGAGAGAAGAAGCAGAG	CTTATTGGCTGCCTGAGTCAAG	[31]
Nestin	GTCCTGGTTCCTGAACTTGTC	GCTTCTTTCTCTACCAGTTCCC	[32]
Vimentin	CTGCTGGAAGGGGAGGAGAG	GGTCATCGTGGTGCTGAGAAG	[32]
GAPDH	TGACGTGGACATCCGCAAAG	CTGGAAGGTGGACAGCGGAGG	[33]

Primer sequences used for the qPCR analysis of intermediate filament proteins.

2.10. Histopathological evaluation

Following decapitation, the left kidney from six animals/group was collected according to standardized necropsy procedures [35], and immediately fixed in 10 % neutral buffered formalin for 96 h. After fixation, the kidneys were cut longitudinally, washed in running distilled water, dehydrated in ascending grades of ethyl alcohol (70–100 %), cleared in two changes of xylene, processed for paraffin embedding and sectioned at five-microns thickness [[36]]. One slide/animal was stained with hematoxylin and eosin, examined microscopically and any histopathological alteration was reported. For lesion scoring, five randomly selected non-overlapped 40× images/slide (thirty images/group) were captured using AmScope microscope digital camera attached to Olympus light microscope. Subsequently, these images were analyzed subjectively for determining the proportions of glomerular congestion, atrophy, and necrosis/images, the proportion of renal tubules suffered cloudy swelling, vacuolar degeneration, pyknosis, necrosis, cast formation, and regeneration in relation to the total numbers of tubules/images, and the frequencies of interstitial congestions, hemorrhage, edema and leukocytic infiltrations/images.

2.11. Data analysis

Data are presented as the mean ± standard error of the mean (SE). All experimental data were subjected to One-way ANOVA followed by Tukey's-B post hoc test for comparison between different groups. $p < 0.05$ was considered statistically significant. All statistical analyses were performed using IBM SPSS 17.0 software (IBM, USA).

3. Results

3.1. GC–MS profile of MOE

The main bioactive chemical constituents identified by GC–MS analysis of MOE are shown in Table 2 and Fig. 1. The data revealed the presence of 24 components with various retention times, belonging to different chemical classes. The major components identified included eugenol (21.56 %), trimethylsilyl palmitate (13.6 %), 7a-isopropenyl- 4,5-dimethyloctahydroinden-4-yl) methanol (10.57 %), 7-acetyl-6-ethyl-1,1,4,4-tetramethyltetralin (5.59 %), menthol (5.01 %), oleic acid trimethylsilyl ester (4.35 %), β-eudesmol (3.84 %), Tau-cadinol (3.81 %), ç-muurolene (3.12) and α-bisabolol oxide A (3.1 %).

3.2. Clinical observations

Animals in the control group and those treated with MOE appeared healthy and no mortalities were recorded. Til-treated and Til/MOE-L groups showed 20 % mortality, while Til/MOE-H group revealed 10 % mortality (Table 3). Both the two groups supplemented with MOE (MOE-L and MOE-H) revealed a significant increase in body weight gain, compared to the control group. Til alone significantly reduced the body weight gain compared to control values. Co-treatment of MOE with Til improved body weight gain only in the Til/MOE-H group, compared with the Til-treated group (Table 3).

Table 2

Bioactive chemical constituents	Chemical Formula	Mass Weight (MW)	Matching Factor (MF)	Retention Time (RT) (min)	Area %
Eugenol: 4-allyl-2-methoxyphenol	$C_{10}H_{12}O_2$	164	951	23.08	21.56
Palmitic acid, TMS derivative: Trimethylsilyl palmitate	$C_{19}H_{40}O_2Si$	328	866	30.52	13.60
7a-Isopropenyl-4,5-dimethyloctahydroinden-4-yl) methanol	$C_{15}H_{26}O$	222	803	23.27	10.57
7-Acetyl-6,-ethyl-1,1,4,4-tetramethyltetralin = Versalide; Ethanone	$C_{18}H_{26}O$	258	911	27.35	5.59
Menthol, 1˙-(butyn-3-one-1-yl)-, (1S,2S,5R): 4-(1-Hydroxy-2-isopropyl-5-methylcyclohexyl)-3-butyn-2 -one	C10H20O2	222	693	21.70	5.01
Oleic acid, trimethylsilyl ester	$C_{21}H_{42}O_2Si$	354	808	31.28	4.35
β-Eudesmol: Eudesm-4(14)-en-11-ol	$C_{15}H_{26}O$	222	927	22.96	3.84
Tau-Cadinol	$C_{15}H_{26}O$	222	900	22.76	3.81
ç-Muurolene	$C_{15}H_{24}$	204	893	22.58	3.12
(-)-.α-Bisabolol oxide A: 2H-Pyran-3-ol, tetrahydro-2,2,6-trimethyl-6-(4-methyl-3-cyclohexen-1-yl)-, [3S[3alpha,6alpha (R*)]]	$C_{15}H_{26}O_2$	236	845	23.72	3.10
1,2-benzenedicarboxylic acid, dioctyl ester	$C_{24}H_{38}O_4$	390	929	39.73	3.05
Sclereodiol	$C_{16}H_{30}O_2$	254	726	25.28	2.44
Anethole: 1-methoxy-4-(1-propenyl)- Benzene	$C_{10}H_{12}O$	148	894	13.39	2.06
Neophytadiene: 1,3-butadiene, 2-(4,812-trimethyltridecyl)-	$C_{20}H_{38}$	278	878	27.10	2.05
Stearic acid, TMS derivative: Trimethylsilyl stearate	$C_{21}H_{44}O_2Si$	356	881	34.37	1.74
Dihydroactinidiolide: 4,4,7a-Trimethyl-5,6,7,7a-tetrahydrobenzofuran-2(4 H)-one	$C_{11}H_{16}O_2$	180	928	20.07	1.57
Palmitic acid, methyl ester	$C_{17}H_{34}O_2$	270	876	28.87	1.57
D- Carvone: 2-Cyclohexen-1-one, 2-methyl-5-(1-methylethenyl)-	$C_{10}H_{14}O$	150	979	12.79	1.12
Hexadecanoic acid	$C_{16}H_{32}O_2$	256	816	29.58	1.09
(-)-Spathulenol:(1aS,4aS,7R,7aS,7bS)-1,1,7-Trimethyl-4-methylenedecahydro-1H-cyclopropa[e] azulen-7-ol	$C_{15}H_{24}O$	220	876	21.29	1.03
13-Heptadecyn-1-ol	$C_{17}H_{32}O$	252	732	27.96	0.90
2-Pentadecanone, 61,014-trimethyl-	$C_{18}H_{36}O$	268	852	27.21	0.75
Farnesene epoxide, E-	$C_{15}H_{24}O$	220	763	19.71	0.72
Cedrene: (3R,3aR,7R,8aS)-3,8,8-Trimethyl-6-methyleneoctahydro-1H-3a,7-methanoazulene	$C_{15}H_{24}$	204	807	18.87	0.66

Bioactive chemical constituents assigned in MOE by GC–MS analysis.

Fig. 1. GC–MS based chemical constituents profiling of MOE.

Table 3
Mortality %, body weight gain, and serum physiological biomarkers in rats in response to single subcutaneous injection of Til (75 mg/kg bw) and oral administration of MOE (400 or 800 mg/kg bw).

	Experimental groups					
	Control	MOE-L	MOE-H	Til	Til/MOE-L	Til/MOE-H
				20		
Parameters						
Mortality (%)	0	0	0		20	10
Body weight gain (gm)	25.50±0.43^{b}	34.66±1.67^{a}	34.50±1.52^{a}	10.83±0.60^{d}	14.16±1.40^{d}	21.00±1.23^{c}
Creatinine (mg/dl)	0.77 ± 0.01^{d}	0.77 ± 0.01^{d}	0.78 ± 0.02^{d}	1.04 ± 0.02^{a}	0.96 ± 0.01^{b}	0.87 ± 0.03^{c}
Urea (mg/dl)	21.50 ± 0.85^{d}	22.67 ± 0.95^{d}	22.00 ± 0.93^{d}	43.83 ± 1.54^{a}	36.17 ± 1.85^{b}	30.33 ± 1.20^{c} Total protein
(gm/dl) 7.39 ± 0.19^{a}	7.52 ± 0.17^{a}	7.16 ± 0.30^{a}	4.14 ± 0.18^{c}	4.47 ± 0.18^{bc}	5.03 ± 0.21^{b} Albumin (gm/dl)	3.88
± 0.10^{a} 4.09 ± 0.07^{a}	4.14 ± 0.09^{a}	2.43 ± 0.07^{c}	2.54 ± 0.17^{c}	3.14 ± 0.15^{b}		
Na (mmol/l)	138.83 ± 3.30^{a}	140.33 ± 3.45^{a}	141.33 ± 2.46^{a}	104.83 ± 1.86^{c}	115.17 ± 1.19^{b}	130.83 ± 2.52^{a}
K (mmol/l)	3.42 ± 0.09^{c}	3.36 ± 0.16^{c}	3.39 ± 0.12^{c}	7.27 ± 0.18^{a}	6.38 ± 0.32^{b}	4.08 ± 0.15^{c}
GGT(U/l)	11.33 ± 0.76^{c}	10.83 ± 0.87^{c}	10.00 ± 0.73^{c}	30.00 ± 1.88^{a}	22.16 ± 1.30^{b}	18.50 ± 0.67^{b}

Means within the same row (in each parameter) carrying different superscripts (a,b,c and d) are significantly different ($p < 0.05$), (mean ± SE). One− way ANOVA followed by Tukey's B post hoc test.
MOE-L: *Moringa oleifera* low dose group.
MOE-H: *Moringa oleifera* high dose group.
Til: Tilmicosin treated group.

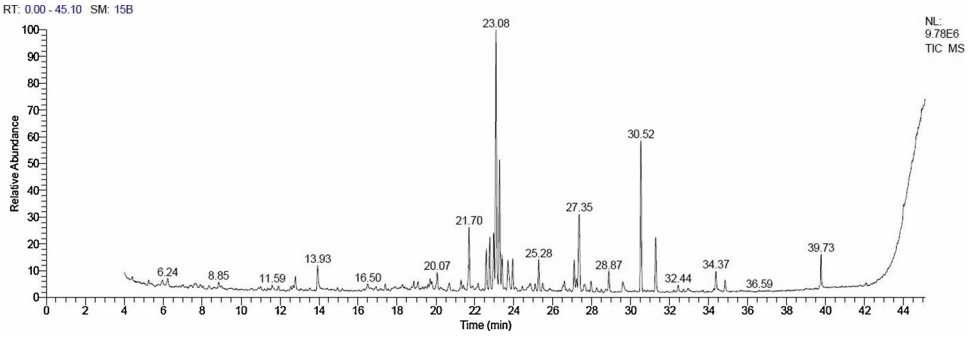

Til/MOE-L: Co treated Tilmicosin /*Moringa oleifera* low dose group.
Til/MOE-H: Co treated Tilmicosin /*Moringa oleifera* high dose group.

3.3. Serum physiological biomarkers

The alterations in serum physiological biomarkers following the administration of Til and/or MOE are shown in Table 3. Animals treated with Til displayed significant increases in serum creatinine, urea, sodium and potassium concentrations, and GGT activity, compared with the control group. On the other hand, serum total protein and albumin levels showed a significant reduction than control values. Treatment of animals with the high dose of MOE concurrently with Til (Til/MOE-H group), improved the alterations in all serum biomarkers, compared to Til group, but the control values were not attained except for serum electrolytes. All biomarkers except total protein and albumin were improved in the Til/MOE-L, compared to the Til group. These findings indicate that the high dose of MOE was more protective than the lower dose.

3.4. Oxidative stress/antioxidants variables

As displayed in Fig. 2, the biomarkers of oxidative stress H_2O_2 and MDA were significantly elevated in renal tissue of the Til-treated rats, compared to the control. The levels of the two parameters were significantly improved by MOE supplementation in both co-treated groups; with the improvement being more prominent in the Til/MOE-H group than in the Til/MOE group. However, the values of the two biomarkers were still significantly higher than control values. The activities of SOD and GPx in the renal tissue showed significant depletion in Til-treated group, compared to the control one. Concurrent treatment of Til- treated animals with MOE significantly recovered enzyme activities, compared to Til group, and the control values were only achieved in the Til/MOE-H group (Fig. 2).

3.5. Inflammatory response markers

Next, we investigated whether inflammation is involved in Til- induced nephrotoxicity by estimating the renal levels of pro- inflammatory cytokines (TNF-α and IL-1β) and comparing values versus the control group. Both biomarkers were increased significantly in the kidneys of Til- treated rats (Fig. 3). MOE administered along with Til, significantly ameliorated the elevations in the two indices, compared to the Til group, with the modulation being more prominent in the Til/MOE-H group than in the Til/MOE-L group. However, the levels were still significantly higher than the control values (Fig. 3).

3.6. Transcription levels of desmin, nestin and vimentin encoding genes

A single administration of Til to rats led to a significant upregulation of the expression of intermediate filament proteins (desmin, nestin and vimentin) in the kidney tissue. In contrast, when MOE was concomitantly administered with Til, it attenuated these alterations, compared to Til-treated animals, especially in the Til/MOE-H. However, in both co-treated groups, the values of gene expression did not return to control values, except for desmin in Til/MOE-H group (Fig. 4).

3.7. Pathological findings

Grossly, the kidneys of control, MOE-L, and MOE-H were apparently normal while those of Til-treated animals were hyperemic and slightly enlarged. Very mild congestions without change in sizes were seen in the kidneys of Til/MOE-L, and Til/MOE-H treated animals. Microscopically, normal histological picture was seen in the renal tissues of the control animals (Fig. 5A). No histopathological alterations were seen in the kidneys of MOE-L, and MOE-H treated animals except for the presence of few eosinophilic debris in the lumens of some renal tubules (Fig. 5B and C). Consistent with the recorded biochemical changes in blood and renal tissue, kidneys of Til-treated animals (Fig. 5D, E and F) exhibited numerous nephropathic alterations, including the glomeruli (congestion, atrophy, lobulation, and necrosis with widening of Bowman's space), tubules (cytoplasmic vacuolation, nuclear pyknosis, attenuation, single-cell necrosis, coagulative necrosis, and cast formation), and the interstitial tissue (congestion with hypertrophied vascular endothelium,

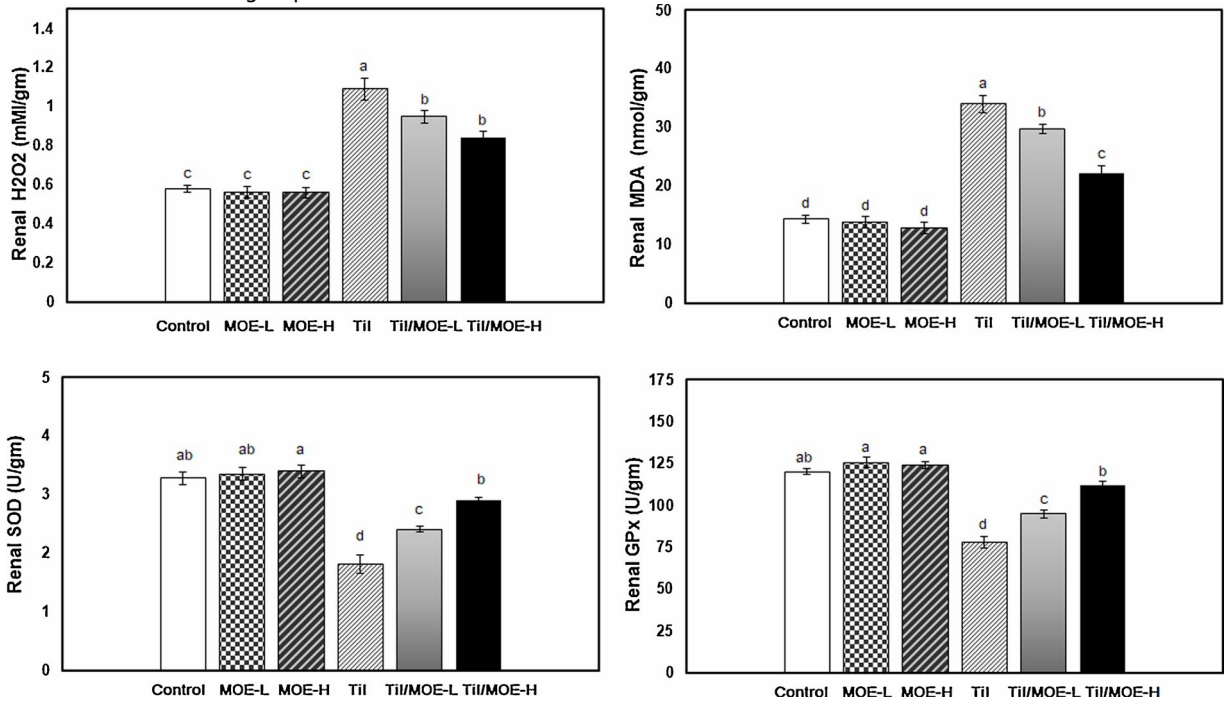

Fig. 2. Oxidative stress and antioxidant variables in the kidney tissue of rats in response to single S/C injection of Til (75 mg/kg bw) and oral administration of MOE (400 or 800 mg/kg bw). One-way ANOVA followed by Tukey's B post hoc test ($P < 0.05$), (mean ± SE). Bars carrying different letters (a,b,c and d) are significantly different. MOE-L: *Moringa oleifera* low dose group, MOE-H: *Moringa oleifera* high dose group, Til: Tilmicosin treated group, Til/MOE-L: Co-treated Tilmicosin/*Moringa oleifera* low dose group, Til/MOE-H: Co-treated Tilmicosin/*Moringa oleifera* high dose group.

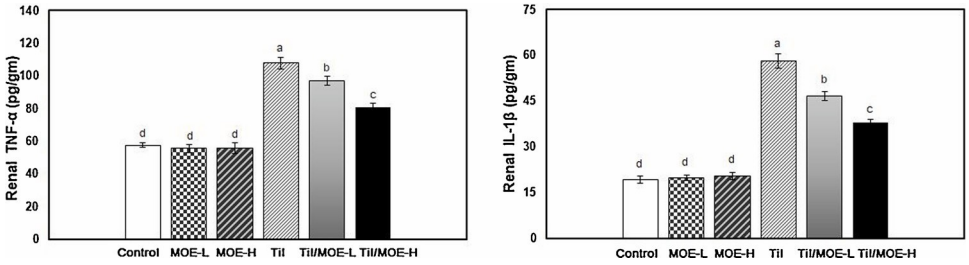

Fig. 3. Inflammatory markers in the kidney tissue of rats in response to single S/C injection of Til (75 mg/kg bw) and oral administration of MOE (400 or 800 mg/kg bw). One-way ANOVA followed by Tukey's B post hoc test ($P < 0.05$), (mean ± SE). Bars carrying different letters (a, b,c and d) are significantly different. MOE-L: *Moringa oleifera* low dose group, MOE-H: *Moringa oleifera* high dose group, Til: Tilmicosin treated group, Til/MOE-L: Co-treated Tilmicosin/*Moringa oleifera* low dose group, Til/MOE- H: Co-treated Tilmicosin/*Moringa oleifera* high dose group.

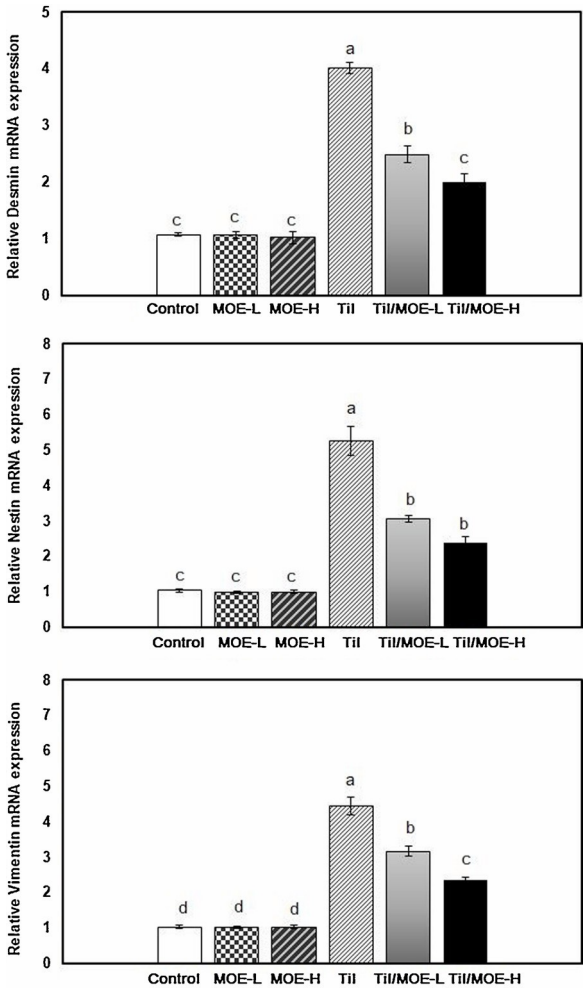
Relative Desmin mRNA expression
Relative Nestin mRNA expression
Relative Vimentin mRNA expression
Control MOE-L MOE-H Til Til/MOE-L Til/MOE-H

Fig. 4. Relative expression of desmin, nestin, and vimentin mRNA in the kidney tissue of rats in response to single S/C injection of Til (75 mg/kg bw) and oral administration of MOE (400 or 800 mg/kg bw). The expression abundance of genes mRNA was normalized against the GAPDH internal control gene. One- way ANOVA followed by Tukey's B post hoc test ($P < 0.05$), (mean ± SE). Bars carrying different letters (a,b,c and d) are significantly different. MOE-L: *Moringa oleifera* low dose group, MOE-H: *Moringa oleifera* high dose group, Til: Tilmicosin treated group, Til/ MOE-L: Co-treated Tilmicosin/*Moringa oleifera* low dose group, Til/ MOE-H: Co-treated Tilmicosin/*Moringa oleifera* high dose group. hemorrhage, edema, and inflammatory cell infiltrates particularly the mononuclear cells).

Supplementation with MOE induced significant nephroprotective effects but did not maintain the normal histology of the renal parenchyma in both the Til/MOE-L, and Til/MOE-H treated animals. Kidneys of the Til/MOE-L treated animals (Fig. 5G, H and I) manifested a significant reduction in the frequencies and severities of the Til-induced nephropathy where most glomeruli showed no morphological alterations except for congestion, and few were collapsed with widen Bowman's space. The tubules largely maintained their normal morphology and numerous tubules showed regenerative epithelium, but few showed epithelial attenuation and single-cell necrosis. The interstitial congestion, hemorrhage, edema, and inflammatory infiltrate were significantly reduced.

Interestingly, kidneys of the Til/MOE-H treated animals (Fig. 5J, K and L) showed a sharp decline in the frequencies and severities of the Til- induced nephropathy as the only reported glomerular alterations were congestion and lobulation. The tubular alterations included cloudy swelling, and cast formation, besides numerous tubules showed regenerative epithelium. The interstitial tissues of some specimens showed vascular congestion and mononuclear cell infiltrations. A quantitative assessment of the renal lesions in all groups was summarized in Table 4. **4. Discussion**

Critical to preventing Til-induced nephrotoxicity is understanding the molecular basis behind its cellular toxicity, and seeking effective protective agents of natural origin. Our data indicate the involvement of oxidative injury, inflammation and upregulation of intermediate filament proteins in the renal injury induced by Til, and the ability of MOE to neutralize these deleterious effects via its antioxidant and anti- inflammatory properties. Herein, a single subcutaneous administration of Til to rats at 75 mg/kg bw induced 20 % mortalities. The main cause of death from Til in various animal species was reported to be cardiac failure, perhaps mediated via depletion of cardiac intracellular calcium [1]. Oxidative damage in vital organs like heart and liver, and the consequent inflammatory response may contribute to the Til-induced mortalities [5, 12]. Co-treatment of MOE with Til failed to reduce mortalities in the Til/MOE-L group, while lowered it to 10 % in the Til/ MOE-H, implying that the protective effect of MOE is dose-dependent.

Our findings revealed reduction of body weight gain in rats treated with Til, which is consistent with the result obtained previously [12]. This could be due to reduced feed and/or water consumption, and/or specific toxic effects inducing metabolic changes which consume the animal energy reserve in combating the effects of the toxicant or in activating repair mechanisms [[37]]. Additionally, it may result from organ degeneration with subsequent breakdown of proteins. Co-treatment of MOE with Til improved the body weight gain, only in the MOE-H group. In addition, administration of MOE alone increased body weight gain in rats. This may be due to the

valuable nutritional components in MO including proteins, minerals, and fatty acids in addition to a plenty of antioxidants which hinder the oxidative injury and stressful consequences induced by Til [12,19]. Additionally, β-Eudesmol, an important component in MOE, has been shown to increase gastric vagal nerve activity in rats, which stimulates appetite and digestion [38].

In this experiment, Til administration was associated with

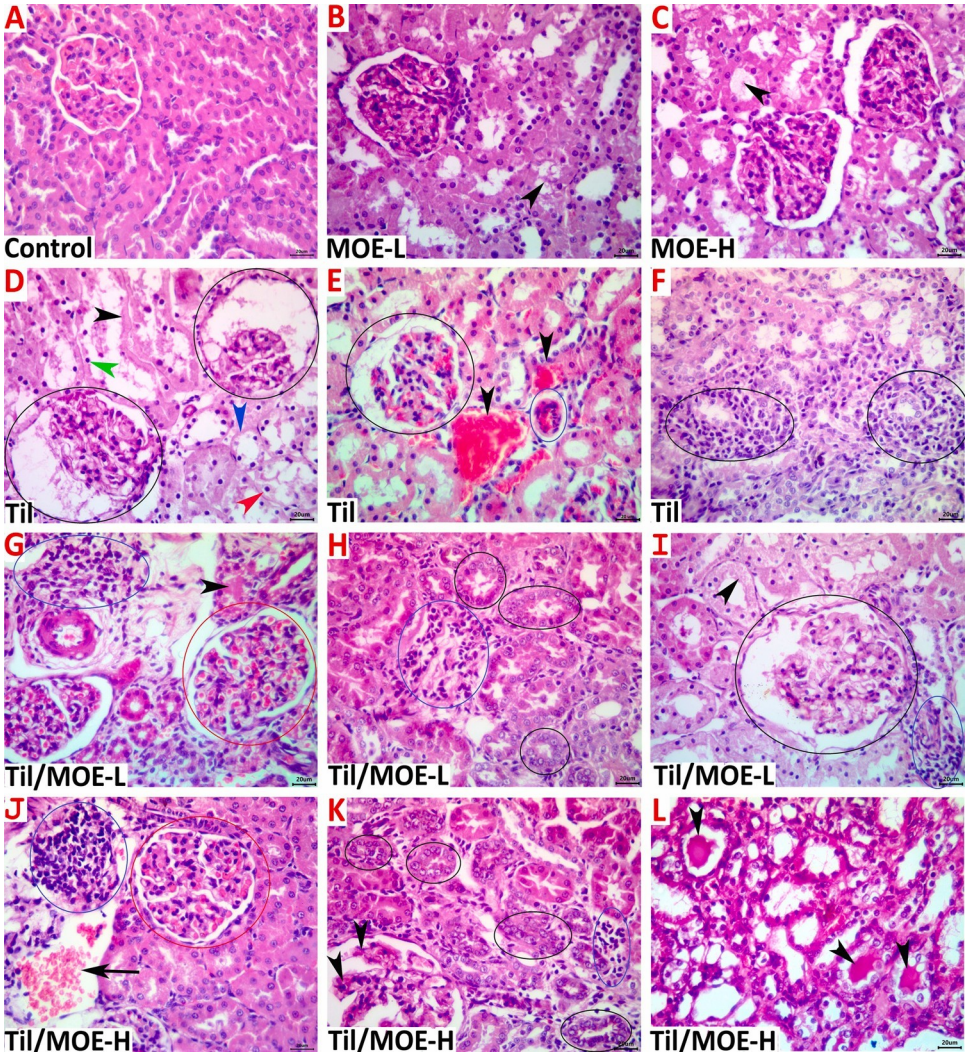

Fig. 5. Representative photomicrograph of H&E stained renal sections showing normal renal corpuscles and tubules (**A**), eosinophilic debris in the lumens of some renal tubules (**B and C**), glomerular necrosis with widen Bowman's space (ellipses), cytoplasmic vacuolation (red arrowhead), nuclear pyknosis (green arrowhead), single-cell necrosis (blue arrowhead), coagulative necrosis (black arrowhead) (**D**), glomerular congestion and collapse (black ellipse), vascular congestion with hypertrophied endothelium (blue ellipse) and congestion (arrowheads) (**E**), interstitial mononuclear cell infiltration (ellipses) (**F**), glomerular congestion (red ellipse), interstitial mononuclear cell infiltration (blue ellipse), hyaline cast (arrow) (**G**), regenerated tubular epithelium (ellipses), interstitial mononuclear cell infiltration (blue ellipse) (**H**), single-cell necrosis (arrowhead), glomerular collapse (black ellipse), interstitial mononuclear cell infiltration (blue ellipse) (**I**), congestion (arrowhead), glomerular congestion (red ellipse), interstitial mononuclear cell infiltration (blue ellipse) (J), glomerular lobulation (arrowheads), regenerated tubular epithelium (black ellipses), interstitial mononuclear cell infiltration (blue ellipse) (**K**), and hyaline casts (arrowheads) (**L**). (Scale bar is 20 μm) (For interpretation of the references to colour in this figure legend, the reader is referred to the web version of this article).

Table 4
Lesion scoring in rat's kidney in response to single subcutaneous injection of Til (75 mg/kg bw) and oral administration of MOE (400 or 800 mg/kg bw).

Parameters	Experimental groups					
				Til		
	Control	MOE-L	MOE-H		Til /MOE-L	Til /MOE-H
Glomerular congestion	$0.00^{c}\pm0.00$	$0.00^{c}\pm0.00$	$0.00^{c}\pm0.00$	46.67 ± 4.22^{a}	26.67 ± 4.22^{b}	20.00 ± 5.16^{b}
Glomerular lobulation	$0.00^{b}\pm0.00$	$0.00^{b}\pm0.00$	$0.00^{b}\pm0.00$	16.67 ± 6.15^{a}	6.67 ± 4.22^{ab}	3.33 ± 3.33^{b}
Glomerular atrophy	$0.00^{b}\pm0.00$	$0.00^{b}\pm0.00$	$0.00^{b}\pm0.00$	20.00 ± 5.16^{a}	6.67 ± 4.22^{b}	0.00 ± 0.00^{b}
Glomerular necrosis	$0.00^{b}\pm0.00$	$0.00^{b}\pm0.00$	$0.00^{b}\pm0.00$	13.33 ± 4.22^{a}	0.00 ± 0.00^{b}	0.00 ± 0.00^{b}
Cloudy swelling	$0.00^{c}\pm0.00$	$0.00^{c}\pm0.00$	$0.00^{c}\pm0.00$	25.00 ± 2.21^{a}	5.58 ± 0.55^{b}	1.45 ± 0.56^{c}
Tubular vacuolation	$0.00^{c}\pm0.00$	$0.00^{c}\pm0.00$	$0.00^{c}\pm0.00$	39.25 ± 2.23^{a}	13.77 ± 4.63^{b}	2.15 ± 0.63^{c}
Tubular pyknosis	$0.00^{b}\pm0.00$	$0.00^{b}\pm0.00$	$0.00^{b}\pm0.00$	23.50 ± 2.82^{a}	1.96 ± 0.61^{b}	0.60 ± 0.27^{b}
Tubular attenuation	$0.00^{b}\pm0.00$	$0.00^{b}\pm0.00$	$0.00^{b}\pm0.00$	17.00 ± 2.32^{a}	2.25 ± 0.35^{b}	0.69 ± 0.31^{b}

Single-cell necrosis	$0.00^{c}\pm0.00$	$0.00^{c}\pm0.00$	$0.00^{c}\pm0.00$	11.82 ± 0.78^{a}	3.69 ± 0.23^{b}	1.55 ± 0.55^{c}
Necrosis	$0.00^{b}\pm0.00$	$0.00^{b}\pm0.00$	$0.00^{b}\pm0.00$	3.29 ± 0.29^{a}	0.21 ± 0.21^{b}	0.00 ± 0.00^{b}
Regenerated tubular epithelium	$0.00^{c}\pm0.00$	$0.00^{c}\pm0.00$	$0.00^{c}\pm0.00$	1.73 ± 0.22^{b}	3.65 ± 0.21^{a}	3.65 ± 0.23^{a}
Cast formation	$0.00^{c}\pm0.00$	$0.00^{c}\pm0.00$	$0.00^{c}\pm0.00$	22.63 ± 1.11^{a}	4.43 ± 0.50^{b}	2.00 ± 0.43^{c}
Interstitial congestion	$0.00^{c}\pm0.00$	$0.00^{c}\pm0.00$	$0.00^{c}\pm0.00$	76.67 ± 6.15^{a}	33.33 ± 6.67^{b}	26.67 ± 4.22^{b}
Interstitial hemorrhage	$0.00^{b}\pm0.00$	$0.00^{b}\pm0.00$	$0.00^{b}\pm0.00$	13.33 ± 4.22^{a}	0.00 ± 0.00^{b}	0.00 ± 0.00^{b}
Interstitial edema	$0.00^{b}\pm0.00$	$0.00^{b}\pm0.00$	$0.00^{b}\pm0.00$	13.33 ± 4.22^{a}	3.33 ± 3.33^{b}	0.00 ± 0.00^{b}
Interstitial inflammatory cell infiltrate	$0.00^{c}\pm0.00$	$0.00^{c}\pm0.00$	$0.00^{c}\pm0.00$	66.67 ± 6.67^{a}	26.67 ± 4.22^{b}	6.67 ± 4.22^{c}

Means within the same row (in each parameter) carrying different superscripts (a, b and c) are significantly different ($p < 0.05$), (mean ± SE). One−way ANOVA followed by Tukey's B post hoc test. MOE− L: *Moringa oleifera* low dose group, MOE-H: *Moringa oleifera* high dose group, Til: Tilmicosin treated group, Til/ MOE-L: Co treated Tilmicosin /*Moringa oleifera* low dose group, Til/ MOE-H: Co treated Tilmicosin /*Moringa oleifera* high dose group.

significantly elevated serum creatinine and urea, as well as reduced total examination of the kidney tissue revealed glomerular congestion, atroprotein and albumin levels, reflecting renal glomerular impairment in phy, lobulation, and necrosis with widen Bowman's space. Similarly, treated rats. In line with these biochemical changes, histomorphological previous reports have indicated glomerular hypertrophy with focal
inflammatory cell infiltration in between glomeruli in mice and broiler chicken treated with Til [7,10]. As creatinine is filtered almost entirely by the glomerulus, and unlike urea it is minimally reabsorbed by renal tubules, it is considered a more reliable marker of impaired glomerular filtration rate (GFR) than urea. A 50 % reduction in GFR will double the serum creatinine concentration [39]. Urea is freely filtered through the glomeruli, and some urea is reabsorbed passively with water in the proximal tubules. Elevation of serum urea level results mainly from reduced glomerular filtration, but the toxic insult to renal tubules and parenchyma may contribute to that increase [40]. Elevated serum creatinine and urea levels were previously reported in Til-treated rats [6], mice [10], and broiler chicken [7]. In contrast, Farag et al. [5] reported that Til elevated serum urea in rats, while creatinine showed no change.

Concerning the alterations in serum protein profile, reduced blood protein may result from suppression of the synthetic function of the liver and/or from glomerular filtration deficit [40]. The increased glomerular permeability with consequent hypoproteinemia and proteinuria may result from oxidative injury and inflammatory response in the cells forming the glomerular filtration barrier [41]. The latter is composed of three layers; glomerular epithelium, the basement membrane, and the slit diaphragms (modified cell-to-cell junctions), which are formed by the interdigitating foot processes of the podocytes. The slit diaphragms have charge and size selective properties making them a molecular sieve and a final barrier preventing passage of proteins and macromolecules into the urinary filtrate [42]. Injury to podocytes by xenobiotics, like Til, affects their complex contractile cytoskeletal actin apparatus, leading to retraction of their foot processes and loss of slit diaphragms, which increases the glomerular permeability and causes runaway proteinuria and nephrotic syndrome [43]. Similarly, these findings agree with the studies conducted previously in rats and mice [5,8].

Moreover, Til-treated rats displayed elevations of serum sodium and potassium levels, and activity of serum GGT, suggesting renal tubular function impairment. In the same context, Til-induced histomorphological changes in renal tubules in the form of cytoplasmic vacuolation, nuclear pyknosis, single-cell necrosis, coagulative necrosis, and cast formation. These are in accordance with previous studies demonstrating histopathological alterations in the renal tubules of Til-treated rats [6], mice [10], and broiler chicken [7]. Elevated blood sodium level results from water depletion due to loss of water in excess of that of sodium and potassium. Renal toxic insult may cause tubular dysfunction (inability to normally concentrate the urine) due to defective Na^{+} reabsorption and unresponsiveness to vasopressin. Additionally, the recorded rise in blood urea level in Til-treated rats may contribute to the observed increase in blood sodium by inducing osmotic diuresis [44]. The glomeruli filter potassium freely, and about 95 % is reabsorbed from the proximal tubules. Meanwhile, potassium is secreted mainly through distal tubules and to some degree by the loop of Henle [40]. Elevation of blood potassium usually results when renal damage reaches the late distal nephron extending into the collecting duct, so that the cells responsible for K + secretion are injured, as in acute tubular necrosis or acute tubulointerstitial nephritis [45].

In rats, GGT is present primarily in kidney, on the brush border cells of the proximal tubules, but also present in liver biliary system, and pancreas. GGT elevation reflects proximal tubular damage and/or cholestasis [46]. Importantly, GGT plays a critical role in cellular antioxidant defense by initiating extracellular glutathione breakdown into its constitutive amino acids. In this way, it provides cysteine, the rate-limiting amino acid for intracellular de novo GSH synthesis. Thus, the elevation of serum GGT level can be attributed to upregulated expression of GGT gene due to increased ROS production in Til-treated rats, in an adaptive response to protect against oxidative stress [47].

Concurrent and post-administration of MOE with Til improved the alterations in all renal function serum biomarkers, except total protein and albumin in the Til/MOE-L group, suggesting that the high dose of MOE is more protective than the lower dose. Interestingly, co-treatment of MOE with Til significantly reduced the frequencies and severities of the Til-induced nephropathic alterations, in a dose-dependent manner. This nephroprotective potential of MOE was previously reported in cobalt, lead and melamine intoxicated rats [23,28,48] and acetaminophen treated mice [49].

The mechanisms underlying Til induced renal insufficiency are not entirely clear. Based on our results, oxidative stress and inflammation emerged as key events in the pathophysiology of Til-induced renal dysfunction. Herein, Til injection induced renal oxidative damage as evidenced by markedly elevated levels of H_2O_2 and the lipid peroxidation marker MDA, accompanied with diminished activities of the antioxidant enzymes SOD and GPx. Our findings coincided with those of Oda and Derbalah [6] in rats, and Kart et al. [50] in mice, where Til injection was associated with elevated renal MDA with tissue GSH depletion. Moreover, Til has been reported to modulate the oxidant/antioxidant status in liver of rats [5,6], and mice [50]. Oxidative stress was also shown to

play a major role in Til induced cardiotoxicity in rats and mice [11,12,50,51].

H_2O_2, a non-radical ROS, is formed by dismutation of superoxide anion radicals by SOD and by direct reduction of oxygen by oxidases. In fact, the elevated renal H_2O_2 in Til-treated rats reflects increased production of ROS in the kidney [41]. This gained support by previous experiments demonstrating that Til increased the level of ROS in heart tissue [11,12] and in liver [5]. H_2O_2 is detoxified rapidly by GPx and CAT, but when H_2O_2 is produced in excess, it may react with iron (Fenton reaction) to generate hydroxyl radical which further propagates the oxidative stress. Because H_2O_2 has membrane transport properties similar to water, unlike superoxide radical, it can easily diffuse out across membranes and influence regulatory systems in other cellular compartments or nearby cells [41].

Reactive oxygen species attack unsaturated fatty acids in cellular membranes and intracellular cytoplasmic components, which accounts for the elevated level of MDA in the renal tissue of Til-treated rats. The depletion of renal antioxidant enzymes (SOD and GPx) indicates the inability of the antioxidant mechanisms to counteract the increased generation of ROS caused by Til [52]. Suppressed SOD and GPx activities may result from increased utilization in detoxication of the generated superoxide radical and H_2O_2, respectively. All renal functions are affected by oxidative stress, including glomerular filtration, tubular reabsorption and secretion in all nephron segments, vascular reactivity and renal hemodynamics (both directly and indirectly). Alteration of these processes and activation of prodamage pathways lead to cellular altered gene expression, necrosis, apoptosis, progression of tissue damage, and abnormal kidney function [41].

Interestingly, co-treatment of MOE with Til reduced H_2O_2 and MDA levels in the kidney homogenate, while improved the activities of SOD and GPx and reduced the frequencies and severities of the Til-induced renal histomorphological lesions. This protective effect was more marked in the MOE-H group. Therefore, the protective effect of MOE seems to be mediated, at least in part, by its antioxidant properties. In agreement with this suggestion, previous studies have reported the ability of MO to offset the oxidative stress and restore the normal antioxidant status in kidney of cobalt, lead and methotrexate intoxicated animals [23,48,53]. Likewise, similar findings were demonstrated in liver [17], heart [12], and brain [21] of Til-treated animals.

The total antioxidant activity of MOE seems to be due to its abundant leave content of natural antioxidants specially polyphenols which have been shown to be potent direct antioxidants in the oxygen radical absorbance capacity assay [54]. Our GC–MS analysis showed that eugenol (4-allyl-2-methoxyphenol) is the main component in MOE constituting 21.56 %. It is a phenolic compound from the class of phenylpropanoids with potent antioxidant activity, reviewed by Barboza et al. [55]. In ABTS and DPPH antioxidant assays, it eliminated 76.9 % and 90.8 % of free radicals, respectively. In another study, it reduced lipid peroxidation and improved the activities of antioxidant enzymes in LPS-mice model. In addition, eugenol showed high singlet oxygen scavenging activity and inhibited superoxide anion production by human neutrophils [56,57]. Palmitic acid methyl derivative (13.6 % in MOE) ameliorated the oxidative stress and improved antioxidant status in CCl4-treated rats [58] and in mice fed on methionine-choline-deficient diet [59]. Moreover, menthol (5.01 % in MOE) protected the brain from β-amyloid peptide toxic insult [60] and prevented carcinogen-induced cutaneous carcinoma in mice by reducing lipid peroxidation and antioxidant depletion [61].

Oleic acid (4.35 % in MOE), is a monounsaturated fatty acid, with one double bond, which makes it less susceptible to oxidation, and thus contributing to its antioxidant activity against oxidative load [62]. It protected rats from cadmium toxicity by reducing endogenous ROS oxidative damage on lipids and proteins, while maintained GSH normal level and increased mitochondrial viability [63]. β-Eudesmol (3.84 % in MOE) has anti-cancer activity by inhibiting superoxide production in human lung (A549) cancer cells [64]. Another important component, α-(-)-Bisabolol (3.1 % in MOE), has potent antioxidant activity reviewed by Kamatou and Viljoen [65]. It displayed nephroprotective effect in vitro through reducing ROS generation and enhancing cell viability in kidney epithelial cells of Rhesus Monkey (LLC-MK2 cells), and in vivo in rat kidney ischemic–reperfusion (I/R) model. Furthermore, anethole (2.06 % in MOE) inhibited lipid peroxidation in vitro [66].

Multiple pathways have been identified that highlight the mechanisms of interplay between inflammation and oxidative stress. Robust body of evidence has demonstrated that oxidative stress is a prime trigger of inflammatory responses. Oxidative stress may cause cellular necrosis and extracellular matrix damage, which in turn release various molecules recognized by pattern recognition receptors (PRRs), and trigger inflammatory cascades [13]. This activates intracellular signaling through transcription factor NF-κB and the molecular platform termed the inflammasome, stimulating production of various inflammatory mediators [15]. Herein, the levels of the pro-inflammatory cytokines TNF-α and IL-1β were markedly upregulated in kidney of Til-treated rats with inflammatory cell infiltration, particularly the mononuclear cells, in the renal interstitial tissue. This raised the concern that inflammation may be involved in propagation of Til-induced renal injury. Our results are in agreement with the previous studies showing TNF-α and IL-1β upregulation in the serum of Til-treated rats [5] and inflammatory cell infiltration in between the glomeruli and tubules of Til-treated mice and broiler chicken [7,10].

In our study, H_2O_2 level was increased in the renal tissue of Til- treated animals, reflecting excess production of ROS which may activate the redox-sensitive NF-κB transcription factor, the master regulator of proinflammatory cytokines, cell division and apoptosis [15]. This suggestion gained confirmation by the previous study of Farag et al. [5] which demonstrated the up-regulation of NF-κB expression by Til in rats. NF-κB activation triggers production of an array of inflammatory cytokines as well as activates pro-oxidant enzyme NADPH oxidase (NOX), which stimulates release of reactive species [15]. As tissue damage and inflammation progress, local tissue and circulating levels of inflammatory mediators such TNF-α and IL-1β continue to increase, NOX in renal cells is further activated, and ROS generation becomes even more evident. In this way, proinflammatory processes and renal tissue injury are amplified causing vascular and cytoskeletal remodeling, fibrosis, and potential renal failure [41].

TNF-α is synthesized and released in the renal tissue by glomerular, tubular epithelial, endothelial and mesangial cells, and infiltrating macrophages. It is a key player in the pathogenesis of kidney injury, triggering inflammation, apoptosis, and the accumulation of extracellular matrix, impairing glomerular blood flow and damaging the glomerular permeability barrier with the development of albuminuria [67]. IL-1β plays a pivotal role in inflammation by causing neutrophil mobilization from the bone marrow (leukocytosis), by activating all types of leukocytes, renal cells and endothelial cells, by triggering fever, and by initiating acute phase response proteins in the liver such as C-reactive

protein. In tissues, it is released mainly by infiltrating macrophages and neutrophils, and resident dendritic cells, whereas parenchymal cells may release only small quantities under certain conditions [68].

Of note, co-treatment of MOE with Til downregulated the TNF-α and IL-1β levels and inhibited inflammatory cell infiltration in renal tissue, in a dose-dependent manner. This indicates that MOE has anti- inflammatory activity which could protect the kidney against Til- induced inflammatory response. Similar activity of MO was previously shown in cobalt and melamine treated rats [23,28] and in acetaminophen intoxicated mice [49]. The major mechanism of action of MO as anti-inflammatory was indicated to be suppression of NF-κB pathway [23,69]. This action of MOE could be attributed to its major components with documented anti-inflammatory effects. Eugenol inhibited expression of COX_2, TNF-α, IL-6, MPO, iNOS, and PGE2, and suppressed the expression of NF-κB signaling and inflammatory cells recruitment in rats and mice [55]. Methyl palmitate reduced NF-κB expression and subsequent production of proinflammatory cytokines in CCl_4-treated rats [58]. In another study, it reduced serum TNF-α and IL-6, and NF-κB expression in the liver and lung tissues of LPS- endotoxemic rats [70].

Menthol diminished TNF-α, IL-1β, IL-6 and MPO activity in acute colitis rat model [71] and prevented carcinogen-induced cutaneous carcinoma in mice by suppressing skin inflammation and hyperplasia, and inhibiting COX2 and NF-κB expression [61]. Oleic acid decreased production of IL-1β, IL-6 and CINC-2αβ (cytokine-induced neutrophil chemoattractant-2 αβ) by rat macrophages [72] and reduced NO, IL-1β, IL-6, and TNF-α production in cadmium intoxicated rats [63]. β-eudesmol downregulated the levels of IL-1β, thymic stromal lymphopoietin, TNF-α, and macrophage inflammatory protein-2, and suppressed level of intercellular adhesion molecule-1 and infiltration of eosinophils. Moreover, it reduced NF-κB DNA binding activity in nasal mucosa tissues in allergic rhinitis mice model [73]. α-(−)-Bisabolol has an anti-inflammatory activity partly due to the suppression of leukotriene synthesis, as it appears to be a good 5-lipoxygenase inhibitor [65]. It was reported to inhibit NLRP3 inflammasome stimulation and TLR4-NFκB/MAPK signaling pathways [74]. Anethole ameliorated acetaminophen hepatotoxicity in mice by downregulating proinflammatory mediators such as NO, TNF-α, IL-1α, MIP-1α and MCP-1 and up-regulating of anti-inflammatory cytokines IL-4 and IL-10 [75]. The main mechanism of action of anethole was reported to be inhibition of NF-κB activation by blocking IκB-α degradation [76]. D-carvone attenuated the lung injury caused by LPS through reducing macrophages and neutrophils in bronchoalveolar lavage fluid and the levels of serum
IL-1β, IL-6 and TNF-α in mice [77].

Among the known cytoskeletal proteins, intermediate filaments (IF) are the most characteristic in podocytes. The IFs form a continuous structural network that extends from the nucleus to the cell periphery. They contribute significantly to the mechanical integrity of cells and play a critical role in many cellular functions such as signal transduction and determination of cell shape and motility [78]. Here, we observed upregulation of the expression the IF proteins desmin, nestin and vimentin in kidney of Til-treated rats. This reflects glomerular podocyte injury accompanied with cellular proliferation and repair [43,79,80]. As shown in previous studies, desmin, nestin and vimentin have been upregulated in kidney of animals treated with different nephrotoxicants including doxorubicin, furan, sodium fluoride, and puromycin aminonucleoside [33,81–83]. In addition, vimentin expression was elevated in ochratoxin-treated mice [84].

Desmin (type III IF protein) upregulation is a sensitive marker of podocyte injury followed by epithelial–mesenchymal transition (EMT) of diseased cells by activating the transforming growth factor-beta (TGF- β1) [85]. The dedifferentiated podocytes loss their highly arborized morphology and adopt a more cobblestone-like morphology [43]. This in turn affects glomerular membrane permeability causing proteinuria [86]. In rat puromycin aminonucleoside nephrosis (PAN) model, desmin was reported to be a valuable and sensitive marker for acute podocyte injury, correlating well with the degree of glomerular damage and albumin/creatinine ratio [83]. Nestin is a type VI IF protein closely associated with vimentin. During development, it is expressed in stem cells in many tissues including the kidney, playing essential role in cell self-renewal/proliferation, differentiation and migration, so it is used as a good stem cell marker [80]. After kidney development (in adults), the expression of nestin is downregulated, but in case of tissue injury, the regeneration process is accompanied with enhanced nestin expression [87]. It has been reported as a marker of podocytes injury followed by repair process and maintenance of the foot process structure [88]. However, other studies have shown that nestin expression was induced in renal tubular and interstitial cells, a process thought to be involved in tissue repair and thus might be used as a marker for tubulointerstitial fibrosis and peritubular endothelial cell injury [79,89].

Despite its importance as a glomerular podocyte injury marker [90], the type III IF protein vimentin was also reported to be a marker of renal tubular damage in rats after ischaemic injury [91] and in human patients with acute kidney injury, where the tubular vimentin was strongly correlated with serum creatinine, urinary N-acetyl-β-D-glucosaminidase, and alpha1-microglobulin and was inversely correlated serum albumin and eGFR [92]. Since vimentin is expressed in metanephric mesenchymal stem cells, which are the progenitors for epithelial cells of the nephron, but not in normally differentiated renal cells, it is used as a good marker of epithelial to mesenchymal transition [84]. Vimentin plays a pivotal role in anchoring and maintaining the cell organelles like mitochondria and hence it is important for energy homeostasis and cellular response to oxidative stress [93]. Co-treatment of animals with MOE ameliorated the effect of Til on the expression of desmin, nestin and vimentin in kidney tissue. This implies that MOE attenuated the cellular toxicity of Til at the level of IF proteins, which further support the protective effect of MOE.

5. Conclusions

Oxidative stress with subsequent inflammatory response and upregulation of intermediate filament protein expression appear to play a key role in mediating Til-induced renal injury. Of note, MOE co- treatment with Til modulated the nephrotoxic effects of Til as evidenced by the improvement of serum biochemical markers, oxidant/ antioxidant status, the evoked inflammatory response and the expression of desmin, nestin and vimentin. Conclusively, the antioxidant and anti-inflammatory potentials of MOE were much more prominent at the higher dose of MOE (800 mg/kg). Based on this mechanistic insight, supplementation of MOE is beneficial in protecting against Til-induced nephrotoxicity. However, further studies are warranted to determine the exact mechanisms of MOE nephroprotective effect.

Funding

This work was funded by Researchers Supporting Project number (RSP-2020/96), King Saud University, Riyadh, Saudi Arabia.

Transparency document

The Transparency document associated with this article can be found in the online version.

Declaration of Competing Interest

The authors declare that there are no conflicts of interest.

Acknowledgments

The authors are grateful to king Saud University, Riyadh, Saudi Arabia, for funding this work through Researchers Supporting Project number (RSP-2020/96).

References

[1] M.G. Papich, Chloramphenicol and derivatives, macrolides, lincosamides, and miscellaneous antimicrobials, in: J.E. Riviere, M.G. Papich 10th (Eds.), Veterinary Pharmacology and Therapeutics, Wiley Blackwell, USA, 2018, pp. 903–952.

[2] M. Zeineldin, J. Lowe, B. Aldridge, Effects of tilmicosin treatment on the nasopharyngeal microbiota of feedlot cattle with respiratory disease during the first week of clinical recovery, Front. Vet. Sci. 7 (2020) 115, https://doi.org/ 10.3389/fvets.2020.00115.

[3] K. Zhou, X. Wang, D. Chen, Y. Yuan, S. Wang, C. Li, Y. Ya, Q. Liu, L. Shao, L. Huang, Z. Yuan, S. Xie, Enhanced treatment effects of tilmicosin against Sstaphylococcus aureus cow mastitis by self-assembly sodium alginate-chitosan nanogel, Pharmaceutics 11 (2019) 524, https://doi.org/10.3390/pharmaceutics11100524. [4] M. Garmyn, K. Vereecken, Gussem De, W. Depondt, F. Haesebrouck, A. Martel, Efficacy of tylosin and tilmicosin against experimental mycoplasma gallisepticum infection in chickens, Avian Dis. 63 (2019) 359–365, https://doi.org/10.1637/ 11991-110818-Reg.1.

[5] M.R. Farag, W.M. Elhady, S.Y.A. Ahmed, H.S.A. Taha, M. Alagawany, Astragalus polysaccharides alleviate tilmicosin-induced toxicity in rats by inhibiting oxidative damage and modulating the expressions of HSP70, NF-kB and Nrf2/HO-1 pathway, Res. Vet. Sci. 124 (2019) 137–148, https://doi.org/10.1016/j.rvsc.2019.03.010.

[6] S.S. Oda, A.E. Derbalah, Impact of diclofenac sodium on tilmicosin-induced acute cardiotoxicity in rats (tilmicosin and diclofenac cardiotoxicity), Cardiovasc. Toxicol. 18 (2018) 63–75, https://doi.org/10.1007/s12012-017-9414-2.

[7] M.A. Rasheed, M. Ashraf, A. Javeed, A.A. Anjum, Toxicological evaluation of tilmicosin after intramuscular injection in broiler chicken, J. Anim. Plant Sci. 28 (2018) 1678–1686.

[8] S. Xie, F. Wang, Y. Wang, L. Zhu, Z. Dong, X. Wang, X. Li, W. Zhou, Acute toxicity study of tilmicosin-loaded hydrogenated castor oil-solid lipid nanoparticles, Part. Fibre Toxicol. 8 (2011) 33, https://doi.org/10.1186/1743-8977-8-33.

[9] X. Zhang, J. Zhu, B. Yang, B. Chen, J. Wu, J. Sha, E. Bao, Transcriptomic investigation reveals toxic damage due to tilmicosin and potential resistance against tilmicosin in primary chicken myocardial cells, Poult. Sci. (2020), https:// doi.org/10.1016/j.psj.2020.08.080.

[10] A. Gheith, A. El-Mahmoudy, S. Elmajdoub, Awidat, Pharmacovigilance of tilmicosin in mice, Acta Sci. Vet. 43 (2015) 1318.

[11] S.R.Khalil Awad, B.M. Hendam, R.M. Abd El-Aziz, M.M. Metwally, T.S. Imam, Protective potency of Astragalus polysaccharides against tilmicosin- induced cardiac injury via targeting oxidative stress and cell apoptosis-encoding pathways in rat, Environ. Sci. Pollut. Res. 27 (2020) 20861–20875, https://doi.org/10.1007/ s11356-020-08565-y.

[12] S.R. Khalil, S.M. Abdel-Motal, M. Abd-Elsalam, N.E. Abd El-Hameed, A. Awad, Restoring strategy of ethanolic extract of Moringa oleifera leaves against Tilmicosin-induced cardiac injury in rats: targeting cell apoptosis-mediated pathways, Gene 730 (2020) 144272, https://doi.org/10.1016/j. gene.2019.144272.

[13] J.K. Chan, J. Roth, J.J. Oppenheim, K.J. Tracey, T. Vogl, M. Feldmann, N. Horwood, J. Nanchahal, Alarmins: awaiting a clinical response, J. Clin. Invest. 122 (2012) 2711–2719, https://doi.org/10.1172/JCI62423.

[14] P. Mukhopadhyay, N. Eid, M.A. Abdelmegeed, A. Sen, Interplay of oxidative stress, inflammation, and autophagy: their role in tissue injury of the heart, liver, and kidney, Oxid. Med. Cell. Longev. (2018) 2090813, https://doi.org/10.1155/2018/ 2090813. PMID: 29765491; PMCID: PMC5885484.

[15] N. Lugrin, R. Rosenblatt-Velin, L. Parapanov, Liaudet, The role of oxidative stress during inflammatory processes, Biol. Chem. 395 (2014) 203–230, https://doi.org/ 10.1515/hsz-2013-0241.

[16] G.G. Moustafa, S.R. Khalil, M.M. Hussein, M. Labib, The cytotoxic and ultrastructural perturbations of aluminum exposed Nile catfish with special reference to the mitigating effect of vitamin C, Life Sci. J. 9 (2012) 5198–5210. [17] S.R. Khalil, H.F. Salem, M.M. Metwally, R.M. Emad, K.M. Elbohi, S.A. Ali, Protective effect of Spirulina platensis against physiological, ultrastructural and cell proliferation damage induced by furan in kidney and liver of rat, Ecotoxicol. Environ. Saf. 192 (2020), 110256.

[18] S.R. Khalil, Y. Abd Elhakim, A.H. Abd El-fattah, M.R. Farag, N.E. Abd El-Hameed, E.M. Abd Elhakeem, Dual immunological and oxidative responses in Oreochromis niloticus fish exposed to lambda cyhalothrin and concurrently fed with Thyme powder (Thymus vulgaris L.): stress and immune encoding gene expression, Fish Shellfish Immunol. 100 (2020) 208–218.

[19] Y. Liu, X. Wang, X. Wei, Z. Gao, J. Han, Values, properties and utility of different parts of Moringa oleifera: an overview, Chinese Herb. Med. 10 (2018) 371–378, https://doi.org/10.1016/j.chmed.2018.09.002.

[20] K.M. Sadek, T.K. Abouzed, R.A. bouelkhair, S. Nasr, The chemo-prophylactic efficacy of an ethanol Moringa oleifera leaf extract against hepatocellular carcinoma in rats, Pharm. Biol. 55 (2017) 1458–1466, https://doi.org/10.1080/ 13880209.2017.1306713.

[21] Mohamed, M. Metwally, S. Khalil, G. Salem, H. Ali, Moringa oleifera extract attenuates the CoCl2 induced hypoxia of rat's brain: expression pattern of HIF-1α, NF-κB, MAO and EPO, Biomed. Pharmacother. 109 (2019) 1688–1697, https://doi. org/10.1016/j.biopha.2018.11.019.

[22] S.R. Khalil, K.M. El Bohi, S. Khater, A.H. Abd El-fattah, F.A. Mahmoud, M.R. Farag, Moringa oleifera leaves ethanolic extract influences DNA damage signaling pathways to protect liver tissue from cobalt-triggered apoptosis in rats, Ecotoxicol. Environ. Saf. 200 (2020), 110716, https://doi.org/10.1016/j.ecoenv.2020.110716.

[23] M.M. Abdel-Daim, S.R. Khalil, A. Awad, E.H. Abu Zeid, R.A. El-Aziz, H.A. El- Serehy, Ethanolic extract of Moringa oleifera leaves influences NF-κB signaling pathway to restore kidney tissue from cobalt-mediated oxidative injury and inflammation in rats, Nutrients 12 (2020) 1031, https://doi.org/10.3390/ nu12041031.

[24] G. Albasher, R. Alrajhi, E. Alshammry, R. Almeer, Moringa oleifera leaf extract attenuates Pb acetate-induced testicular damage in rats, Comb. Chem. High Throughput Screen. (2020), https://doi.org/10.2174/1386207323666200923142831. Epub ahead of print.

[25] Y.J. Li, Q.Q. Ji, Z. Wang, L.H. Shen, B. He, Moringa oleifera seeds mitigate myocardial injury and prevent ventricular failure induced by myocardial infarction, Am. J. Transl. Res. 12 (2020) 4511–4521.

[26] M.Saleem Saleem, M.F. Akhtar, Antioxidant, anti-inflammatory and antiarthritic potential of Moringa oleifera Lam: an ethnomedicinal plant of Moringaceae family, South Afr. J. Bot. 128 (2020) 246–256, https://doi.org/10.1016/j.sajb.2019.11.023.

[27] Mabrouki, I. Rjeibi, J. Taleb, L. Zourgui, Cardiac ameliorative effect of moringa oleifera leaf Extract in high-fat diet-induced obesity in rat model, Biomed Res. Int. (2020) 6583603, https://doi.org/10.1155/2020/6583603.

[28] Y.M. Abd-Elhakim, W.A.M. Mohamed, K.M. El.Bohi, H.A. Ali, F.A. Mahmoud, T. M. Saber, Prevention of melamine-induced hepatorenal impairment by an ethanolic extract of Moringa oleifera: changes in KIM-1, TIMP-1, oxidative stress, apoptosis, and inflammation-related genes, Gene 764 (2021), 145083, https://doi. org/10.1016/j.gene.2020.145083.

[29] R.C. Wiggins, The spectrum of podocytopathies: a unifying view of glomerular diseases, Kidney Int. 71 (2007) 1205–1214, https://doi.org/10.1038/sj. ki.5002222.

[30] F. Scheubert, S. Hufsky, Bocker, Computational mass spectrometry for small ¨ molecules, J. Cheminformatics. 5 (2013) 12, https://doi.org/10.1186/1758-2946- 5-12.

[31] J.O. Goncalves, A.C.A. Tannuri, M.C.M. Coelho, I. Bendit, U. Tannuri, Dynamic expression of desmin, α-SMA and TGF-β1 during hepatic fibrogenesis induced by selective bile duct ligation in young rats, Braz. J. Med. Biol. Res. 47 (2014) 850–857, https://doi.org/10.1590/1414-431X20143679.

[32] G. Luna, G.P. Lewis, C.D. Banna, O. Skalli, S.K. Fisher, Expression profiles of nestin and synemin in reactive astrocytes and Müller cells following retinal injury: a comparison with glial fibrillar acidic protein and vimentin, Mol. Vis. 16 (2010) 2511–2523.

[33] A. Awad, S.R. Khalil, M.R. Farag, M.A. Nassan, Differential susceptibility of kidneys and livers to proliferative processes and transcriptional level of the genes encoding desmin, vimentin, connexin 43, and nestin in rats exposed to furan, Ecotoxicol. Environ. Saf. 162 (2018) 235–244, https://doi.org/10.1016/j.ecoenv.2018.07.003.

[34] K.J. Livak, T.D. Schmittgen, Analysis of relative gene expression data using realtime. Quantitative PCR and the 2-DDCT method, Method. 25 (2001) 402–408. [35] C. Ruehl-Fehlert, B. Kittel, G. Morawietz, P. Deslex, C. Keenan, C.R. Mahrt, T. Nolte, M. Robinson, B.P. Stuart, U. Deschl, Revised guides for organ sampling and trimming in rats and mice-Part

1, Exp. Toxicol. Pathol. 55 (2003) 91–106, https://doi.org/10.1078/0940-2993-00311.
[36] K.S. Suvarna, C. Layton, J.D. Bancroft, Bancroft's theory and practice of histological techniques E-Book, Elsevier Health Sciences (2018).
[37] S.R. Khalil, A. Awad, H.H. Mohammed, Behavioral response and gene expression changes in fipronil-administered male Japanese quail (Coturnix japonica), Environ. Poll. 223 (2017) 51–61, https://doi.org/10.1016/j.envpol.2016.12.027.
[38] K. Ohara, T. Fukuda, Y. Ishida, C.K. Takahashi, R. Ohya, M. Katayama, K. Uchida, M. Tominaga, K. Nagai, β-Eudesmol, an oxygenized sesquiterpene, stimulates appetite via TRPA1 and the autonomic nervous system, Sci. Rep. 7 (2017) 15785, https://doi.org/10.1038/s41598-017-16150-16156.
[39] J.E. Whalan, Clinical chemistry. A Toxicologist's Guide to Clinical Pathology in Animals, Springer International Publishing, Switzerland, 2015, pp. 67–94.
[40] G.O. Evans, Animal Clinical Chemistry: a Practical Handbook for Toxicologists and Biomedical Researchers, 2nd ed., CRC Press, Boca Raton, USA, 2009.
[41] B.B. Ratliff, W. Abdulmahdi, R. Pawar, M.S. Wolin, Oxidant mechanisms in renal injury and disease, Antioxid. Redox Signal. 25 (2016) 119–146, https://doi.org/ 10.1089/ars.2016.6665.
[42] P.A. Garg, Review of podocyte biology, Am. J. Nephrol. 47 (Suppl.1) (2018) 3–13, https://doi.org/10.1159/000481633.
[43] C.J. May, M. Saleem, G.I. Welsh, Podocyte dedifferentiation: a specialized process for a specialized cell, Front Endocrinol, (Lausanne). 5 (2014) 148, https://doi.org/ 10.3389/fendo.2014.00148.
[44] R. Sam, P. Hart, R. Haghighat, T.S. Ing, Hypervolemic hypernatremia in patients recovering from acute kidney injury in the intensive care unit, Clin. Exp. Nephrol. 16 (2012) 136–146, https://doi.org/10.1007/s10157-011-0537-7.
[45] B.F. Palmer, D.J. Clegg, Hyperkalemia across the continuum of kidney function, Clin. J. Am. Soc. Nephrol. 13 (2018) 155–157, https://doi.org/10.2215/ CJN.09340817.
[46] T. Sasikala, A.R. Bitla, A. Sachan, Urinary brush border enzymes for early diagnosis of tubular dysfunction in patients with type 2 diabetes mellitus, Int. J. Res. Med. Sci 7 (2019) 2015–2021, https://doi.org/10.18203/2320-6012.ijrms20192475.
[47] H. Zhang, H.J. Forman, Redox regulation of gamma-glutamyl transpeptidase, Am. J. Respir. Cell Mol. Biol. 41 (2009) 509–515, https://doi.org/10.1165/rcmb.2009- 0169TR.
[48] M.M. Abdel-Daim, S. Alkahtani, R.A. Almeer, G. Albasher, Alleviation of lead acetate-induced nephrotoxicity by Moringa oleifera extract in rats: highlighting the antioxidant, anti-inflammatory, and anti-apoptotic activities, Environ. Sci. Pollut. Res. Int. (2020), https://doi.org/10.1007/s11356-020-09643-x.
[49] G. Karthivashan, A.U. Kura, P. Arulselvan, N.M. Isa, S. Fakurazi, The modulatory effect of Moringa oleifera leaf extract on endogenous antioxidant systems and inflammatory markers in an acetaminophen-induced nephrotoxic mice model, PeerJ 4 (2016) e2127, https://doi.org/10.7717/peerj.2127.
[50] Kart, M. Karapehlivan, K. Yapar, M. Citil, A. Akpinar, Protection through L- carnitine on tissue oxidant status and sialic acid content in tilmicosin-induced alterations in BALB/c Mice, Acta Vet. Brno. 76 (2007) 203–207, https://doi.org/ 10.2754/avb200776020203.
[51] Aboubakr, F. Elsayd, A. Soliman, S.E. Fadl, A. El-Shafey, E.Y. Abdelhiee, L- Carnitine and vitamin E ameliorate cardiotoxicity induced by tilmicosin in rats, Environ. Sci. Pollut. Res. Int. 27 (2020) 23026–23034, https://doi.org/10.1007/ s11356-020-08919-6.
[52] E. Yazar, V. Altunok, M. Elmas, B. Tras¸, A.L. Bas¸, V. Ozdemir, The effect of tilmicosin on cardiac superoxide dismutase and glutathione peroxidase activities, J. Vet. Med. B Infect. Dis. Vet. Public Health 49 (2002) 209–210, https://doi.org/10.1046/j.1439-0450.2002.00545.x.
[53] Soliman, A. Aldhahrani, A. Alkhedaide, M. Nassan, F. Althobaiti, W. Mohamed, The ameliorative impacts of Moringa oleifera leaf extract against oxidative stress and methotrexate-induced hepatorenal dysfunction, Biomed. Pharmacother. 128 (2020) 110259, https://doi.org/10.1016/j.biopha.2020.110259.
[54] T.B. Tumer, P. Rojas-Silva, A. Poulev, I. Raskin, C. Waterman, Direct and indirect antioxidant activity of polyphenol-and isothiocyanate-enriched fractions from Moringa oleifera, J. Agr. Food Chem. 63 (2015) 1505–1513, https://doi.org/ 10.1021/jf505014n.
[55] J.N. Barboza, C. da Silva Maia Bezerra Filho, R.O. Silva, J.V.R. Medeiros, D.P. de Sousa, An overview on the anti-inflammatory potential and antioxidant profile of eugenol, Oxid. Med. Cell. Longev. (2018), 3957262, https://doi.org/10.1155/ 2018/3957262.
[56] Y. Sueishi, R. Nii, Comparative profiling of clove extract and its component antioxidant activities against five reactive oxygen species using multiple free radical scavenging, Food Sci. Technol. Res. 25 (2019) 885–890, https://doi.org/ 10.3136/fstr.25.885.
[57] Chniguir, C. Pintard, D. Liu, P.M.C. Dang, J. El-Benna, R. Bachoual, Eugenol prevents fMLF-induced superoxide anion production in human neutrophils by inhibiting ERK1/2 signaling pathway and p47phox phosphorylation, Sci. Rep. 9 (2019) 18540, https://doi.org/10.1038/s41598-019-55043-8.
[58] E.M. Mantawy, M.G. Tadros, A.S. Awad, D.A. Hassan, E. El-Demerdash, Insights antifibrotic mechanism of methyl palmitate: impact on nuclear factor kappa B and proinflammatory cytokines, Toxicol. Appl. Pharmacol. 258 (2012) 134–144, https://doi.org/10.1016/j.taap.2011.10.016.
[59] L. Zhang, H.X. Li, W.S. Pan, F. Khan, C. Qian, F.R. Qi-Li, X. Xu, Administration of methyl palmitate prevents non-alcoholic steatohepatitis (NASH) by induction of PPAR-α, Biomed. Pharmacother. 111 (2019) 99–108, https://doi.org/10.1016/j. biopha.2018.12.059.
[60] M. Bhadania, H. Joshi, P. Patel, V.H. Kulkarni, Protective effect of menthol on β-amyloid peptide induced cognitive deficits in mice, Eur. J. Pharmacol. 681 (2012) 50–54, https://doi.org/10.1016/j.ejphar.2012.01.035.
[61] Z. Liu, C. Shen, Y. Tao, S. Wang, Z. Wei, Y. Cao, H. Wu, F. Fan, C. Lin, Y. Shan, P. Zhu, L. Sun, C. Chen, A. Wang, S. Zheng, Y. Lu, Chemopreventive efficacy of menthol on carcinogen-induced cutaneous carcinoma through inhibition of inflammation and oxidative stress in mice, Food Chem. Toxicol. 82 (2015) 12–18, https://doi.org/10.1016/j.fct.2015.04.025.
[62] R.W. Owen, R. Haubner, G. Würtele, E. Hull, B. Spiegelhalder, H. Bartsch, Olives and olive oil in cancer prevention, Eur. J. Cancer Prev. 13 (2004) 319–326, https:// doi.org/10.1097/01.cej.0000130221.19480.7e.
[63] B. Bhattacharjee, P.K. Pal, A. Chattopadhyay, D. Bandyopadhyay, Oleic acid protects against cadmium induced cardiac and hepatic tissue injury in male Wistar rats: a mechanistic study, Life Sci. 244 (2020), 117324, https://doi.org/10.1016/j. lfs.2020.117324.
[64] M. Ben Sghaier, M. Mousslim, A. Pagano, Y. Ammari, J. Luis, H. Kovacic, β-eudesmol, a sesquiterpene from Teucrium ramosissimum, inhibits superoxide production, proliferation, adhesion and migration of human tumor cell, Environ. Toxicol. Pharmacol. 46 (2016) 227–233, https://doi.org/10.1016/j. etap.2016.07.019.
[65] G.P.P. Kamatou, A.M. Viljoen, A review of the application and pharmacological properties of α-bisabolol and α-bisabolol-rich oils, J. Am. Oil Chem. Soc. 87 (2010) 1–7, https://doi.org/10.1007/s11746-009-1483-3.
[66] S. Aazza, B. Lyoussi, M.G. Miguel, Antioxidant and antiacetylcholinesterase activities of some commercial essential oils and their major compounds, Molecules 16 (2011) 7672–7690, https://doi.org/10.3390/molecules16097672.
[67] M.D. Sanchez-Nino, A. Benito-Martin, S. Gonçalves, A. Sanz, A. Ucero,˜ M. Izquierdo, A. Ramos, S. Berzal, R. Selgas, M. Ruiz-Ortega, J. Egido, A. Ortiz, TNF superfamily: a growing saga of kidney injury modulators, Mediators Inflamm. (2010) 182958, https:// doi.org/10.1155/2010/182958 •.
[68] H.J. Anders, Of inflammasomes and alarmins: IL-1β and IL-1α in kidney disease, J. Am. Soc. Nephrol. JASN 27 (2016) 2564–2575, https://doi.org/10.1681/ ASN.2016020177.
[69] N.Z. Rani, K. Husain, E. Kumolosasi, Moringa genus: a review of phytochemistry and pharmacology, Front. Pharmacol. 9 (2018) 108–133, https://doi.org/ 10.3389/fphar.2018.00108.
[70] N.M. Saeed, E. El-Demerdash, H.M. Abdel-Rahman, M.M. Algandaby, F.A. Al- Abbasi, A.B. Abdel-Naim, Anti-inflammatory activity of methyl palmitate and ethyl palmitate in different experimental rat models, Toxicol. Appl. Pharmacol. 264 (2012) 84–93, https://doi.org/10.1016/j.taap.2012.07.020.
[71] M. Ghasemi-Pirbaluti, E. Motaghi, H. Bozorgi, The effect of menthol on acute experimental colitis in rats, Eur. J. Pharmacol. 805 (2017) 101–107, https://doi. org/10.1016/j.ejphar.2017.03.003.
[72] J. Magdalon, M.A. Vinolo, H.G. Rodrigues, V. Paschoal, R. Torres, J. Filho, P. Calder, E. Hatanaka, R. Curi, Oral administration of oleic or linoleic acids modulates the production of inflammatory mediators by rat macrophages, Lipids 47 (2012) 803–812, https://doi.org/10.1007/s11745-012-3687-9.
[73] P.D. Moon, N.R. Han, J.S. Lee, H.Y. Kim, S. Hong, H.J. Kim, M.S. Yoo, H.M. Kim, H. J. Jeong, β-eudesmol inhibits thymic stromal lymphopoietin through blockade of caspase-1/NF-κB signal cascade in allergic rhinitis murine model, Chem. Biol. Interact. 294 (2018) 101–106, https://doi.org/10.1016/j.cbi.2018.08.026.
[74] M.F. Nagoor Meeran, S. Azimullah, F. Laham, S. Tariq, S.N. Goyal, E. Adeghate, S. Ojha, α-Bisabolol protects against β-adrenergic agonist-induced myocardial infarction in rats by attenuating inflammation, lysosomal dysfunction, NLRP3 inflammasome activation and modulating autophagic flux, Food Funct. 11 (2020) 965–976, https://doi.org/10.1039/c9fo00530g.
[75] B. Rocha, A. Ritter, F. Ames, O. Gonçalves, F. Leimann, L. Bracht, M. Natali, R. Cuman, C. Bersani-Amado, Acetaminophen-induced hepatotoxicity: preventive effect of trans anethole, Biomed. Pharmacother. 86 (2017) 213–220, https://doi.org/10.1016/j.biopha.2016.12.014.
[76] Kang, K.Y. Kim, H.S. Lee, S.S. Min, G.H. Seol, Anti-inflammatory effects of anethole in lipopolysaccharide-induced acute lung injury in mice, Life Sci. 93 (2013) 955–961, https://doi.org/10.1016/j.lfs.2013.10.014.
[77] M. Zhao, J. Du, Anti-inflammatory and protective effects of D-carvone on lipopolysaccharide (LPS)-induced acute lung injury in mice, J. King

Saud Univ. - Sci. 32 (2019) 1592–1596, https://doi.org/10.1016/j.jksus.2019.12.016.
[78] L. Chang, R.D. Goldman, Intermediate filaments mediate cytoskeletal crosstalk, Nat. Rev. Mol. Cell Biol. 5 (2004) 601–613, https://doi.org/10.1038/nrm1438.
[79] D. Wen, L. Ni, L. You, L. Zhang, Y. Gu, C. Hao, J. Chen, Upregulation of nestin in proximal tubules may participate in cell migration during renal repair, Am. J. Physiol. Renal Physiol. 303 (2012) F1534–F1544, https://doi.org/10.1152/ ajprenal.00083.2012.
[80] Bernal, L. Arranz, Nestin-expressing progenitor cells: function, identity and therapeutic implications, Cell. Mol. Life Sci. 75 (2018) 2177–2195, https://doi. org/10.1007/s00018-018-2794-z.
[81] S.R. Khalil, A.T. Mohammed, A.H. Abd El-Fattah, A.W. Zaglool, Intermediate filament protein expression pattern and inflammatory response changes in kidneys of rats receiving doxorubicin chemotherapy and quercetin, Toxicol. Lett. 288 (2018) 89–98, https://doi.org/10.1016/j.toxlet.2018.02.024.
[82] T.M. Saber, M.F. Mansour, A.S. Abdelaziz, R.M.S. Mohamed, R.A. Fouad, A. H. Arisha, Argan oil ameliorates sodium fluoride-induced renal damage via inhibiting oxidative damage, inflammation, and intermediate filament protein expression in male rats, Environ. Sci. Pollut. Res. 27 (2020) 30426–30436, https:// doi.org/10.1007/s11356-020-09366-z.
[83] Herrmann, E. Tozzo, J. Funk, Semi-automated quantitative image analysis of podocyte desmin immunoreactivity as a sensitive marker for acute glomerular damage in the rat puromycin aminonucleoside nephrosis (PAN) model, Exp. Toxicol. Pathol. 64 (2012) 45–49, https://doi.org/10.1016/j.etp.2010.06.004.
[84] Loboda, A. Stachurska, P. Podkalicka, M. Sobczak, O. Mucha, A. Witalisz-Siepracka, A. Jozkowicz, J. Dulak, Effect of heme oxygenase-1 on ochratoxin A- ´ induced nephrotoxicity in mice, Int. J. Biochem. Cell Biol. 84 (2017) 46–57, https://doi.org/10.1016/j.biocel.2017.01.003.
[85] Y. Liu, Renal fibrosis: new insights into the pathogenesis and therapeutics, Kidney Int. 69 (2006) 213–217, https://doi.org/10.1038/sj.ki.5000054.
[86] Y. Li, Y.S. Kang, C. Dai, L.P. Kiss, X. Wen, Y. Liu, Epithelial-to-mesenchymal transition is a potential pathway leading to podocyte dysfunction and proteinuria, Am. J. Pathol. 172 (2008) 299–308, https://doi.org/10.2353/ajpath.2008.070057. [87] Wiese, A. Rolletschek, G. Kania, P. Blyszczuk, K.V. Tarasov, Y. Tarasova, R. P. Wersto, K.R. Boheler, A.M. Wobus, Nestin expression - a property of multi- lineage progenitor cells? Cell, Cell. Mol. Life Sci. 61 (2004) 2510–2522, https:// doi.org/10.1007/s00018-004-4144-6.
[88] N. Wagner, K.D. Wagner, H. Scholz, A. Schedl, K.M. Kirschner, Intermediate filament protein nestin is expressed in developing kidney and heart and might be regulated by the Wilms' tumor suppressor Wt1, Am. J. Physiol. Regul. Integr. Comp. Physiol. 291 (2006) R779–R787, https://doi.org/10.1152/ ajpregu.00219.2006.
[89] M. Tomioka, K. Hiromura, T. Sakairi, S. Takeuchi, A. Maeshima, Y. Kaneko, T. Kuroiwa, T. Takeuchi, Y. Nojima, Nestin is a novel marker for renal tubulointerstitial injury in immunoglobulin A nephropathy, Nephrol. 15 (2010) 568–574, https://doi.org/10.1111/j.1440-1797.2010.01342.x.
[90] J. Zou, T.H. Chang, H. Chang, E. Yaoita, Y. Yoshida, M. Nameta, T. Yamamoto, X. Jin, Time course of expression of intermediate filament protein vimentin, nestin and desmin in rat renal glomerular injury, Chin. Med. J. 120 (2007) 1203–1205, https://doi.org/10.1097/00029330-200707010-00018.
[91] G. Toubeau, D. Nonclercq, J. Zanen, G. Laurent, P.R. Schaudies, J.A. Heuson- Stiennon, Renal tissue expression of EGF and EGF receptor after ischaemic tubular injury: an immunohistochemical study, Exp. Nephrol. 2 (1994) 229–239. [92] Y. Fujigaki, Y. Tamura, M. Nagura, S. Arai, T. Ota, S. Shibata, F. Kondo, Y. Yamaguch, S. Uchida, Unique proximal tubular cell injury and the development of acute kidney injury in adult patients with minimal change nephrotic syndrome, BMC Nephrol. 18 (2017) 339, https://doi.org/10.1186/s12882-017-0756-6.
[93] I.S. Chernoivanenko, E.A. Matveeva, V.I. Gelfand, R.D. Goldman, A.A. Minin, Mitochondrial membrane potential is regulated by vimentin intermediate filaments, FASEB J. 29 (2015) 820–827, https://doi.org/10.1096/fj.14-259903.